Chemical Engineering Journal 225 (2013) 164–173

Contents lists available at SciVerse ScienceDirect

Chemical Engineering Journal

journal homepage: www.elsevier.com/locate/cej

CuO/SBA-15 catalyst for the catalytic ozonation of mesoxalic and oxalic acids. Water matrix effects

A.L. Petre [a], J.B. Carbajo [a], R. Rosal [a,b], E. Garcia-Calvo [a,b], J.A. Perdigón-Melón [a,*]

[a] Department of Analytical Chemistry and Chemical Engineering, University of Alcalá, E-28871 Alcalá de Henares, Madrid, Spain
[b] Advanced Study Institute of Madrid, IMDEA-Agua, Parque Científico Tecnológico, E-28805 Alcalá de Henares, Madrid, Spain

HIGHLIGHTS

- Catalytic ozonation of organic acids using CuO/SBA-15 as catalyst was studied.
- The effect of inorganic anions on the ozonation process was determined.
- The non-catalytic process was severely affected. Catalytic ozonation was almost unaffected.
- Under non-catalytic ozonation in STP effluent, oxalic acid was depleted by precipitation.
- Under catalytic ozonation in STP effluent, oxalate was depleted by ozone oxidation.

ARTICLE INFO

Article history:
Received 25 October 2012
Received in revised form 8 February 2013
Accepted 11 March 2013
Available online 25 March 2013

Keywords:
Silica-based ordered mesoporous materials
Copper oxide
Ozonation
Oxalic and mesoxalic acids
Wastewater

ABSTRACT

The depletion of mesoxalic and oxalic acids, two of the main by-products of wastewater ozone treatment, was studied in non-catalytic and catalytic ozonation using copper oxide supported on mesoporous silica SBA-15 as catalyst. The influence of the main inorganic anions present in natural and STP effluents (bicarbonates, sulphates, chlorides and phosphates) was also studied. The non-catalytic reaction rate was strongly dependent on the presence of inorganic anions and it was also almost inhibited by the presence of particulate material. Catalysed ozonation not only accelerates organic acid depletion, but was almost unaffected by the presence of these inorganic anions, or by the presence of suspended solids. The efficiency of catalytic and non-catalytic ozonation for depletion of both acids was studied in a real STP effluent. The depletion of mesoxalic acid was considerably slowed down in non-catalysed reactions, whereas under catalysed conditions it was not affected. Oxalate depletion was dominated by the formation with calcium of an insoluble salt, the precipitation equilibrium of which reversed only in the presence of a catalyst.

1. Introduction

Ozonation treatment is one of the most highly recommended technologies for the removal of refractory compounds in wastewater treatment [1]. Due to its high oxidation potential and disinfectant power, ozone is used in drinking water treatment and in water reclamation processes [2–4]. However homogeneous ozonation alone is generally unable to reduce the content of dissolved organic carbon, and it is generally assumed that for reclaimed water, the presence of organic matter is one of the main limiting factors [5]. Its inability to achieve organic carbon mineralisation leads to the accumulation of residual organic by-products, which mainly consist of aldehydes and low molecular weight organic acids [6,7]. These compounds are considered like assimilable organic carbon (AOC), so they should be eliminated in water reuse applications in order to avoid undesirable bacterial re-growth which could present several problems in the use of reclaimed water, such as health concerns (opportunistic pathogens), corrosion, biofouling or aesthetic deterioration of water [8–10].

The elimination of refractory compounds by ozonation has been studied through the use of advanced oxidation processes (AOPs). These are designed to produce a relatively high concentration of hydroxyl radicals, a species with higher oxidation potential. Several ozone mediated AOPs have been developed, the most widely studied for wastewater treatment being O_3/UV and O_3/H_2O_2 [11]. These processes present several drawbacks, such as a reduced efficiency in the presence of particulate materials and radical scavengers and the high cost of supplying hydrogen peroxide or UV radiation [1,12,13]. The ozonation rate of organic compounds is largely determined by the nature of the water matrix [14,15]. Superficial and sewage treatment plant (STP) effluents present a complex mixture of microorganisms, suspended solids (TSS) and organic and inorganic compounds that strongly influence the

* Corresponding author. Tel.: +34 918 856 393.
E-mail address: ja.perdigon@uah.es (J.A. Perdigón-Melón).

1385-8947/$ - see front matter © 2013 Elsevier B.V. All rights reserved.
http://dx.doi.org/10.1016/j.cej.2013.03.071

reaction rate of target compounds. In surface water and wastewater, the concentrations of such compounds are normally several orders of magnitude greater than that of target compounds and thus, although their kinetic constants are lower, their influence should be considered. Special care must be taken in the oxidation of ozone refractory compounds, for which the presence of hydroxyl radicals is required. It is well known that some relatively abundant compounds can act as radical scavengers, notably affecting the reaction rate [14–16].

Catalytic ozonation is an emerging technology that can achieve the total mineralisation of organic compounds, overcoming the previously mentioned drawbacks of AOP technologies. Different catalysts have been studied either in homogeneous and heterogeneous phase [1,7,9,16]. From a technological and practical point of view, heterogeneous catalysts present the clear advantage of being much easier to recover, generally by precipitation or filtration, with the possibility of repeated catalyst reuse. Heterogeneous catalytic ozonation presents some particular features in comparison to other catalytic processes, the main one being the need to monitor catalyst stability. Although the leaching of active phases is always undesirable, the use of metals in water treatment might compromise water reuse if the metals enter the treated water, eventually exceeding discharge limits [17]. Another aspect to take into consideration in catalytic water ozonation is that the main inorganic anions found in surface water and STP effluent, such as chloride, sulphates and phosphates, are commonly poisons for the catalysts blocking the active catalytic sites. The most frequently used catalysts in ozonation are those based on manganese, copper, alumina, titanium and iron oxides as well as activated carbon, which acts as a radical promoter and support [12,16,18–24].

The family of highly ordered siliceous mesoporous materials have attracted great attention due to their important applications in a wide variety of fields such as separation, catalysis, adsorption and advanced nanomaterials, with the result that the number of synthesised materials is continuously increasing [25–27]. These materials present a narrow pore size distribution and a high surface area and pore volume, rendering periodic mesoporous silicas promising supports for metal and metal oxide catalysts. Among these materials, SBA-15 [28] has been intensively studied. This material presents a periodically ordered structure, which consists of two dimensional hexagonal arrays of uniform mesopores [29]. The main features of SBA-15 materials with respect to other ordered mesoporous silicas include its larger and tailored mesoporous pore diameter (control of pore size by synthesis temperature from 3 to 20 nm [30]) and thicker walls (approx. 4 nm), which confer higher mechanical and thermal stability [28].

In this study, we examined the catalytic and non-catalytic ozonation of two refractory by-products, namely oxalic and mesoxalic acids, which are the usual by-products of ozonation of larger organic molecules. We used copper oxide supported on mesoporous solid SBA-15 as the catalyst for heterogeneous ozonation. The effect of working pH, the concentration of the main inorganic anions present in wastewaters and the presence of suspended solids were also studied. In addition, we performed runs in a real effluent obtained from the secondary clarifier of a STP.

2. Material and methods

2.1. Materials

Pluronic P123 (Aldrich $EO_{20}PO_{70}EO_{20}$, EO ethylene oxide, PO propylene oxide, MW = 5800) and tetraethoxysilane (TEOS 98% GC Aldrich) were used as received. Silica SBA-15 was prepared according to a method reported in the literature [31]. In a typical synthesis, 6 g of Pluronic P123 was dissolved in 45 g of water and 180 g of 2 M HCl solution and stirred at 308 K until total dissolution. TEOS (12.5 g) was added to that solution and stirred at 308 K for 20 h. The mixture was then aged at 373 K for 24 h. The white powder was recovered by filtration, washed with water and dried at 323 K overnight. The product was calcined at 773 K for 12 h with a heating rate of 1 K/min. Impregnation of SBA-15 was carried out by the minimum volume method. In a typical impregnation, 2.0 g of the copper precursor, cupric nitrate trihydrate (Fluka), was dissolved in 30 mL of water, and this solution was slowly poured over 5 g of calcined SBA-15 while stirring. The stirring was maintained for 10 h and the solid dried at 323 K overnight. The catalyst was activated by calcination under air flow at 773 K for 8 h with a heating rate of 1 K/min.

The powder X-ray diffraction patterns of the calcined catalyst were collected on X-ray diffractometer Polycristal X'pert Pro PANalytical which employed Ni-filtered Cu Kα (λ = 1.5406 nm) radiation and was operated at 0.02°/min, 40 kV and 40 mA. The scanning range of small-angle pattern was 2θ = 0.6–4° with a step size of 0.02° and a counting time of 20 s per step. The quantitative wide-angle XRD spectrum was recorded over the 2θ range 4–90° with a step size of 0.02° and counting time of 50 s per step.

N_2 adsorption–desorption isotherms measured at −77 K using a Beckman Coulter SA 3100. Copper content was determined by Inductively Coupled Plasma-Mass Spectrometry using a quadrupole mass spectrometer Agilent 7700X operating after complete catalyst dissolution in the hot acid media. Diffuse reflectance UV–vis spectra were recorded on a Shimadzu UV-2550 PC spectrophotometer equipped with a Harrick Praying Mantis™ diffuse reflection accessory. The spectra were recorded under air-exposed conditions in the range of 900–190 nm with a resolution of 0.2 nm. The reflectance of anhydrous KBr was used as reference. The reflectance data were converted by the instrument software to the Kubelka–Munk function $F(R\infty)$ values according to the Kubelka–Munk theory. Zeta potential was measured with a Malvern Zetasizer Nano ZS (Malvern Instruments, UK) with 633 nm He–Ne laser equipped with an MPT-2 Autotitrator by a potentiometric titration performed with 0.25 mol/L HCl from pH = 12 to pH = 2, at 298 K.

Wastewater samples were taken from the output of the secondary clarifier of a STP located in Alcalá de Henares (Madrid). This plant treats a mixture of domestic and industrial wastewater from some facilities located near the city and has a nominal capacity of 3000 m^3/h. The biological treatment uses a conventional A2O configuration with nitrification–denitrification and enhanced phosphorus removal. Details can be found elsewhere [32]. All samples were immediately processed or stored in a refrigerator (<269 K) inside glass bottles. The main physicochemical parameters of the wastewater are summarised in Table 1.

2.2. Experimental procedure

The reaction was carried out in semi-batch conditions in a 1 L double jacketed Pyrex reactor by continuously bubbling a mixture of ozone/oxygen (ozone concentration 25 g/m^3) through a porous glass disk at a flow rate of 0.2 m^3/h. The ozone was generated using a corona discharge ozonator Ozomatic SW 100 from oxygen supplied by a PSA Airsep AS-12 unit. The working temperature was

Table 1
Main physicochemical parameters of Alcala de Henares STP effluent.

		Anions (mg/L)		Cations (mg/L)	
PH	7.7	NO_3^-	36	Na^+	83
COD (mg/L)	27	PO_4^{3-}	1.2	NH_4^+	3.3
TOC (mg/L)	8.1	SO_4^{2-}	82	K^+	15
Turbidity (NTU)	5.3	Cl^-	83	Mg^{2+}	20
Conductivity (μS/cm)	667			Ca^{2+}	32
TSS (mg/L)	7.3				

maintained at 298 K with a Huber polystat cc2 thermostat. The pH of the reaction was measured and controlled with a Crison electrode connected to a Eutech Cybernetycs αpH1000 controller, which delivered a 0.1 M NaOH solution by activating a LC 10AS Shimadzu pump. The concentration of ozone in the gas phase was measured using a non-dispersive UV Photometer Anseros Ozomat GM6000 Pro calibrated and tested using the Potassium Iodide Method (SM 2350 E). The ozone concentration in the liquid was measured using a Rosemount 499A OZ amperometric analyser equipped with Pt 100 RTD temperature compensation and calibrated using the Indigo Colorimetric Method (SM 4500-O3 B). The signal was transmitted to a Rosemount 1055 SoluComp II Dual Input Analyser. The signals from the dissolved ozone concentration, pH and temperature were monitored and recorded using an Agilent 34970 Data Acquisition Unit connected to a computer. The reaction vessel was agitated at 400 rpm with a four-arms propeller. In all runs, the ozone/oxygen mixture was bubbled though 950 mL of the reaction matrix until attaining a constant value for dissolved ozone concentration (4.5 ± 0.6 mg/L). Afterwards, 50 mL of a solution containing 1000 mg/L of oxalate (oxalic acid disodium salt) and 1000 mg/L of mesoxalate (mesoxalic acid disodium salt monohydrate) was added to achieve an initial concentration of both acids of 50 mg/L. Samples were withdrawn at prescribed intervals and the ozone was quenched prior to analysis. In catalysed reactions, 0.5 g of catalyst (≈0.055 g of CuO) was added and kept in ozonated water for at least 30 min to allow the catalyst surface to attain equilibrium prior to the addition of acids. After ozone quenching, samples were filtered using a 0.45 μm Teflon filter to separate the catalyst. Samples were analysed immediately after being obtained.

2.3. Analyses

The concentration of oxalic and mesoxalic acid as well as that of the inorganic anions was determined using ion chromatography in a Dionex DX-120 apparatus equipped with an IonPac AS9-HC 4 × 250 mm analytical column and an AG9-HC 4 × 50 mm guard column. The mobile phase was 9 mM $NaHCO_3$ with a flow rate of 1 mL/min. Cations were also measured by ion chromatography using Metrohm advanced compact IC equipment with a Metrosep C3 4 × 250 mm column and a C3 guard column. The mobile phase was 3.5 mM HNO_3. The concentration of leached copper was measured by a colorimetric method using Merck kit 1.14767.0001 (range of applicability 0.02–6.00 mg/L). Absorbance was measured at 605 nm in a double beam spectrophotometer Shimadzu UV-1800. In order to avoid possible interferences of other species present in the water, the spectrophotometer reference used was a sample of the same water matrix.

3. Results and discussion

3.1. Catalyst characterisation

Nitrogen adsorption–desorption isotherms of the catalyst exhibit type IV isotherms according to IUPAC classification with H1 hysteresis loop (Fig. 1a), which is characteristic of mesoporous materials with one-dimensional cylindrical channels. The sharpness of the increase in the adsorbed nitrogen volume in the adsorption branch of the isotherm due to capillary condensation within the mesopores, indicates the uniformity of mesopores in the sample [29,33]. The catalyst presents a BET specific surface area of 643 m^2/g and a mean pore diameter of 7.6 nm calculated with Barrett–Joyner–Halenda (BJH) method.

The low-angle XRD diffraction pattern of the catalyst (Fig. 1b) present three well-resolved diffraction peaks which corresponds to the diffraction of (100), (110) and (200) planes, these peaks are characteristic of the hexagonally ordered (p6mm) structure of SBA-15 [29].

The amount of supported copper was 8.9 wt.% (11.2 wt.% as CuO) close to the expected value of 10 wt.%. The powder XRD patterns in the wide-angle region (4–90°) (Fig. 1c) shows a broad diffraction peak at 24° which indicates the amorphous nature of SBA-15 [34] and a sharp and well defined diffraction pattern. All the peaks on the XRD pattern can be indexed to that of the monoclinic CuO according to the literature (JCPDS, file No 80-1916) [35]. Based on the XRD pattern average particle size can be estimated using Debye–Scherrer formula giving a size of 33 nm. This large and well crystallized copper oxide phase supported on SBA-15 is normally found with copper oxide loadings higher than 4.5% and catalysts calcined at high temperature [36].

The UV–vis diffuse reflectance spectroscopy is known to be a very sensitive probe for the identification and characterisation of metal ion coordination and it has been used extensively to characterize the coordination environment of Cu^{2+} ions in mesoporous materials. Fig. 1d shows the diffuse reflectance UV–vis spectrum for CuO/SBA-15 sample. Two different bands can be observed; a broad band between 540 nm and 890 nm, centered at about 750 nm and a narrow one centered at 234 nm. The first absorption band are normally assigned to d–d transitions of Cu^{2+} ions in a pseudo-octahedral ligand oxygen environment, which is assigned to copper species in the extra-framework position (CuO particles). The second absorption band at 235 nm, is assigned to the charge transfer transition of the ligand O^{2-} to mononuclear metal centre Cu^{2+}. This band is normally associated with the incorporation of copper cation to the SBA-15 framework [34,37–40].

The PZC of the catalysts was 2.7 (Fig. 1e). Nevertheless, according to XRD and UV–vis diffuse reflectance data catalyst surface should present two separately phases, the support itself and the metal oxide. Surface zeta potential of SBA-15 and commercial copper oxide (Sigma–Aldrich) have been measured separately (Fig. 1e). Bare SBA-15 gives a PZC of 2.4 meanwhile copper oxide gives a higher value of 9.7, both values similar to those found in the literature [40–43]. The similitude between catalyst and SBA-15 is probably due to the poor copper oxide dispersion onto support surface.

3.2. Consumed ozone

A typical profile of ozone evolution is shown in Fig. 2. The initial constant value of dissolved ozone (before the addition of organic acids) corresponds to the equilibrium between the rate of ozone transfer from the gas phase and the rate of ozone decomposition in the liquid phase. After the addition of an organic compound (reaction time 0 in Fig. 2), a sharp reduction of ozone concentration takes places due to its reaction with organic acids. The concentration of dissolved ozone reaches a minimum and then subsequently increases. Eventually, after total depletion of the oxidisable organic matter, the initial ozone concentration is restored. The initial ozone depletion is caused by a rapid reaction with oxidisable organic matter, the ozone demand of which exceeds ozone transfer from the gas phase. Once the more easily oxidisable organic matter is depleted, continuous ozone transfer forces an increase in the concentration. The shadowed area in Fig. 2 represents the ozone dose transferred to the liquid and consumed during the reaction. This amount can be calculated according to the following equation:

$$m_{O_3} = \int_0^t (1-\epsilon_g) V k_L a \left(C^*_{O_3} - C_{O_3}\right) dt = (1-\epsilon_g) V k_L a \left(C^*_{O_3} t - \int_0^t C_{O_3} dt\right) \quad (1)$$

where ϵ is the gas hold-up and V the working volume. In our case, $(1-\epsilon_g)V = 1L$, k_La is the individual mass transfer coefficient, $C^*_{O_3}$

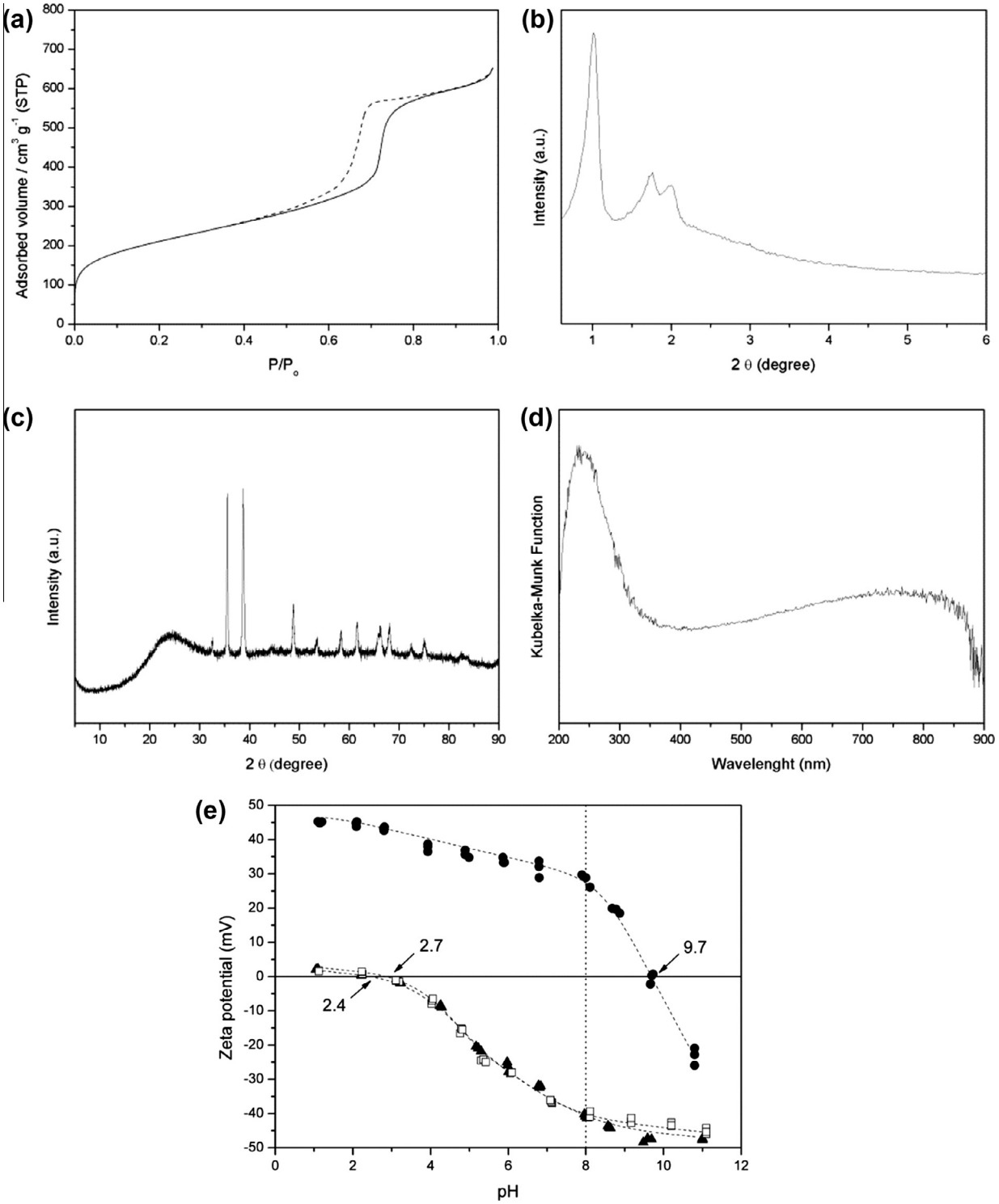

Fig. 1. Catalyst characterisation: (a) N_2 adsorption–desorption isotherm, (b) low-angle X-ray diffraction pattern, (c) wide-angle X-ray diffraction data, (d) UV–vis diffuse reflectance spectrum of CuO/SBA-15 powder and (e) zeta potential and PZC of CuO/SBA-15 (□), SBA-15 (▲) and CuO (●). The measurements were conducted in 55 mg/L aqueous solutions at 298 K.

was determined by the Henry law and $\int_0^t C_{O_3} dt$ was calculated from the registered ozone profile as indicated in Fig. 2 and the preceding paragraph. By comparing the ozone transferred in the presence ($m_{O_3}^{org}$) and absence ($m_{O_3}^{o}$) of organic matter under same working conditions, the amount of ozone consumed by the organic acids was estimated. Eq. (2) summaries this calculation, in which the last parenthesis corresponds to the shadowed area in Fig. 2:

$$\begin{aligned} m_{O_3}^{org} - m_{O_3}^{o} &= \int_0^t (1-\epsilon_g) V k_L a \left(C_{O_3}^{*} - C_{O_3}^{org} \right) dt \\ &\quad - \int_0^t (1-\epsilon_g) V k_L a (C_{O_3}^{*} - C_{O_3}^{0}) dt \\ &= (1-\epsilon_g) V k_L a \left(\int_0^t C_{O_3}^{0} dt - \int_0^t C_{O_3}^{org} dt \right) \end{aligned} \quad (2)$$

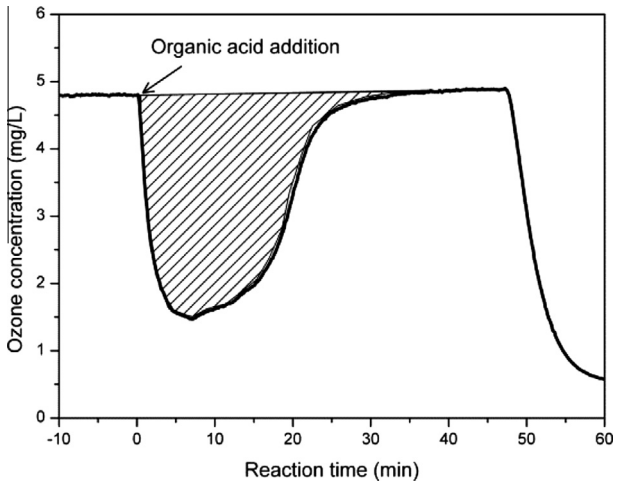

Fig. 2. Generic ozone concentration profile.

3.3. Influence of pH

Fig. 3 shows the evolution of the concentration of oxalic and mesoxalic acids in a binary mixture (initial concentration of 50 mg/L each) ozonated at different pH levels and in the presence and absence of catalyst (CuO/SBA-15, 0.5 g). In non-catalytic reactions (filled symbols) the degradation rate of both compounds was faster at higher pH values. At pH 3 and 5 only a slight depletion (less than 10%) of the target compounds was observed after 30 min. In contrast, at pH 8, total depletion of mesoxalic and oxalic acids was achieved in 15 and 30 min, respectively. Ozone reactions are strongly influenced by pH. At low pH the reaction with molecular ozone is known to be the main reaction pathway, while at basic pH the indirect reaction, through hydroxyl radicals generated from the decomposition of ozone, dominates [44–47]. This result suggests that both acids are mainly eliminated by the indirect oxidation pathway, in agreement with some authors who have reported that oxalic acid does not react readily with molecular ozone and reacts relatively slowly with hydroxyl radicals [20,48]. In addition, pH also affects the ozonation rate of organic acids because of their degree of dissociation. It has been reported that deprotonated acids react several orders of magnitude faster than their protonated forms [45]. At pH 8, organic acids (oxalic acid $pK_{a,1} = 1.27$ and $pK_{a,2} = 4.27$, mesoxalic acid $pK_{a,2} = 3.6$) are fully deprotonated. It is reasonable to assume that both factors contribute to the faster depletion of oxalic and mesoxalic acids at basic pH. Similar results have previously been reported [21].

Mesoxalic acid reacted more readily than oxalic acid under all tested conditions. In fact, in non-catalysed reactions at pH 8, the concentration of oxalic acid remained essentially unchanged until the total depletion of mesoxalic acid (Fig. 3c). This result fits well with the above-mentioned ozone depletion profile, in the first part of which there was a sharp decrease in ozone concentration. This would correspond to the reaction of the more reactive mesoxalic acid, after which the oxidation of the more refractory oxalic acid takes place. Catalysed reactions displayed the same general trend, but with some important differences. Mesoxalic acid was more readily oxidised than oxalic acid at the three pH levels studied. For both acids, the higher the pH the higher the rate of depletion, but the catalysed reaction was considerably enhanced at low pH with respect to non-catalytic ozonation. At pH 3, depletion after 30 min reached values of 89% and 57% for mesoxalic and oxalic acid, respectively, and 100% and 85% at pH 5. At pH 8, the total depletion of mesoxalic and oxalic acid was achieved after 10 and 20 min, respectively, representing a one third reduction in total reaction time with respect to the non-catalytic reaction and thus indicating a good performance of the catalyst. At pH 8, the concentration of mesoxalic acid rapidly decreased during the first part of the reaction, whereas the concentration of oxalic acid initially remained constant but then its concentration increased to over 10%. Fig. 4 shows the evolution of molar concentrations of oxalic and mesoxalic acids as well as the total molar concentration of both. During the first part of the non-catalysed reaction, oxalic acid concentration was constant while the sum of the two acids decreased in parallel to mesoxalic acid depletion. In the catalysed reaction, the sum of both concentrations initially decreased with mesoxalic depletion, but before the mesoxalic acid was completely eliminated, a plateau was reached, corresponding to an increase in oxalic concentration. This result suggests the presence of another reaction pathway in addition to the indirect mechanism, in which mesoxalic acid is partially oxidised to oxalic acid as a result of catalytic ozonation. Similar results have been found by other authors during the catalytic oxidation of tartronic acid to mesoxalic acid with air [49]. These authors have reported that at low pH, tartronic acid oxidises to mesoxalic acid, but at pH 8 mesoxalic acid is readily oxidised to oxalic acid. Mesoxalic acid probably forms germinal diols which would be easily oxidised on the catalyst surface to yield oxalic acid and CO_2. It has also been shown that the rate of oxidation of germinal diols increases with pH [50].

It is well known that pH strongly influences the stability of supported metallic catalysts due to the leaching of active phase. It can be seen that at pH 8, the copper concentration in water was low, accounting for less than 0.36 mg/L (0.8% of the total copper). However, at acidic pH the concentration of leached copper was as high as 15 mg/L (≈40% of the total active phase). The presence of dissolved copper can increase the rate of the homogeneous catalytic reaction, which could contribute to accelerating the decomposition of oxalic acid [16,21].

Heterogeneous catalytic ozonation may involve other non-oxidative depletion mechanisms such as the precipitation of insoluble compounds or the adsorption of reactive species on the catalyst surface. Adsorption experiments using the same experimental conditions but without ozone were carried out and yielded a reduction of only 5% and 8% in the total concentration of oxalic and mesoxalic acids after 30 min. Similar adsorption experiments carried out with bare SBA-15 shown that neither oxalic nor mesoxalic acid are adsorbed onto the support surface. This fact could be expected taking into account that at the working pH = 8 the SBA-15 surface is negatively charged (zeta potential of −40 mV, Fig. 1e) and considering the electrostatic interactions between the deprotonated carboxylic acid species and the surface sites the adsorption should be hindered [40,51]. Nevertheless, this pH is lower than copper oxide pH_{PZC} so its surface should be positively charged (zeta potential + 35 mV) and the adsorption of these molecules onto the copper oxide should be enhanced [42]. In addition to adsorption the capacity of dicarboxilic organic acid complexation with copper oxide should be considered, in the study of organic matter oxidation with copper oxide based catalysts, the formation of a stable copper oxalate phase at the surface of the catalysts has been reported, this phase plays a main role in catalytic pathway and/or catalyst stability [16,52,53]. According to this data the low adsorbed amount of organic acid founded on the catalyst surface should take place onto copper oxide crystal, the low adsorbed amount is due to the poor dispersion of this phase. This suggests that initial mesoxalic and oxalic acid depletion is probably due to the oxidation mechanism rather than to adsorption or precipitation.

Two main mechanisms for catalytic ozonation have been proposed in the literature. One is the decomposition of ozone by metal ions, yielding a high concentration of hydroxyl radicals. The other is the formation of a complex between the catalyst and organic

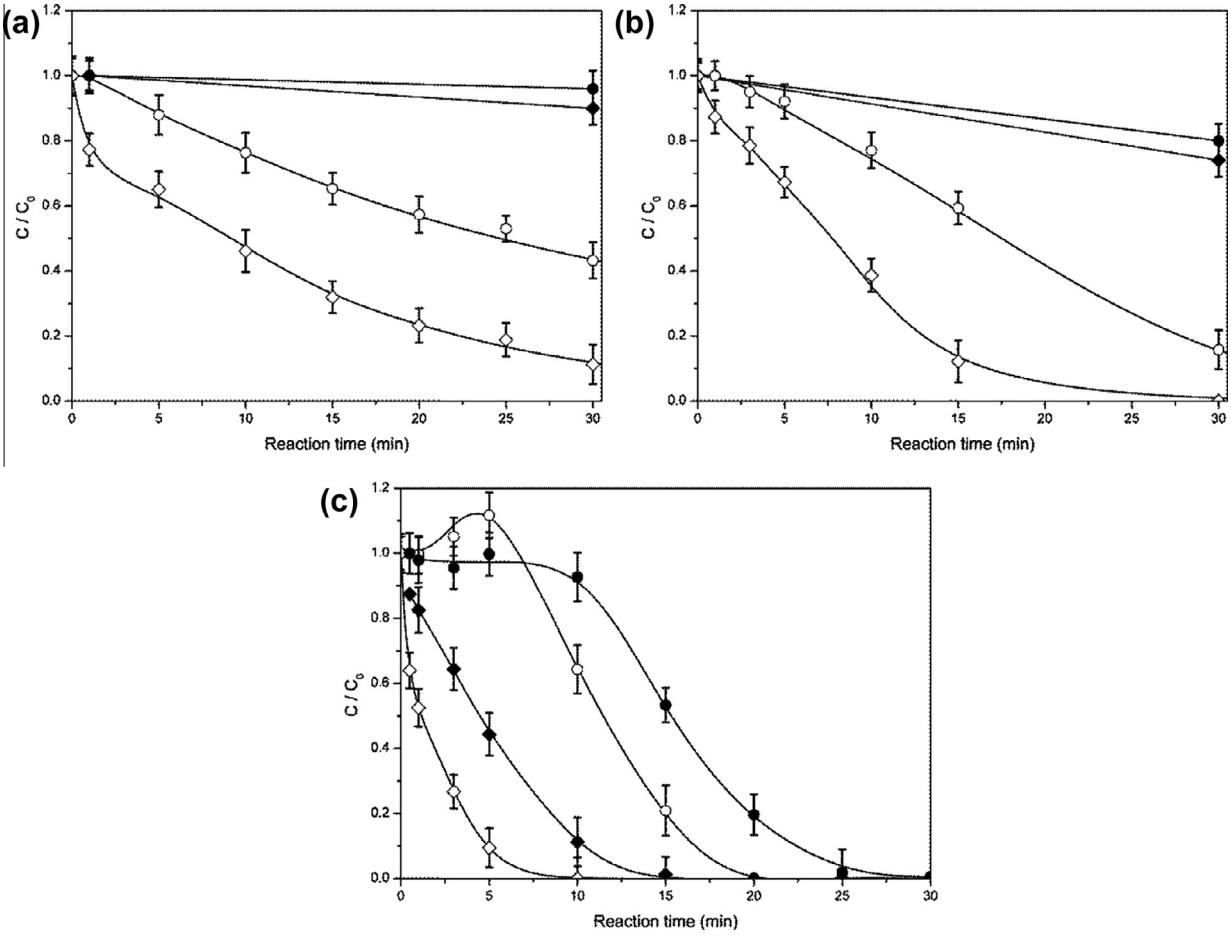

Fig. 3. Evolution of mesoxalic (♦ non-catalysed; ◇ catalysed) and oxalic acid (● non-catalysed; ○ catalysed) concentration at: (a) pH = 3, (b) pH = 5, (c) pH = 8. Error bars represent the standard deviation of sample replicates.

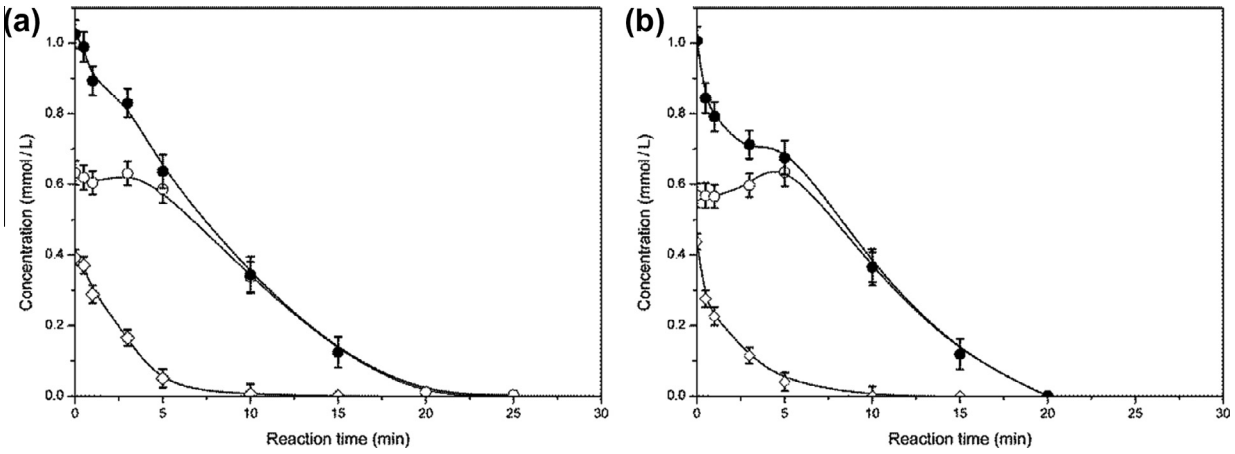

Fig. 4. Time evolution of the molar concentration of mesoxalic acid (◇), oxalic acid (○) and sum of both (●) at pH = 8 in non-catalysed reaction (a) and catalysed reaction (b). Error bars represent the standard deviation of sample replicates.

molecules, followed by oxidation of the former [18,19,54,55]. In order to obtain an insight into the reaction mechanism, the influence of the catalyst on the kinetics of ozone decomposition at pH 8 was studied. The data fit well ($r > 0.999$) with a first order reaction, the pseudo-first order rate constant 0.19 min^{-1} in non-catalysed reaction and 0.25 min^{-1} in catalytic one are similar, indicating that catalysts do not initiate ozone decomposition to form hydroxyl radicals [1,12]. This result suggests that the catalytic reaction occurs mainly through complexation/adsorption mechanism. This could explain the partial oxidation of mesoxalic acid to oxalic acid in the catalytic runs.

3.4. Influence of inorganic anions

The individual influence of the four main inorganic anions present in STP effluent, bicarbonate, phosphate, chloride and sulphate,

Table 2
Influence of the inorganic anions in the reactions parameters obtained at pH 8 and 298 K.

	Component		Mesoxalic[a]		Oxalic[a]		Molar ratio
Catalysed	Anion/source	Concentration (mg/L)	50%	100%	50%	100%	O_3/organic acid
No			4.5	15	15	30	2.2
Yes			1.3	10	11.4	25	2.1
No	HCO_3^-/$NaHCO_3$	250	12.7	>30	25	>30	2.9
Yes			1.3	10	11.4	25	2.5
No	PO_4^{3-} / NaH_2PO_4	1[b]	7.7	30	21.2	30	2.3
Yes			1.5	15	15.6	30	2.2
No	Cl^-/NaCl	100	10.7	25	24	>30	2.5
Yes			2.5	25	11.8	25	2.1
No	SO_4^{2-}/Na_2SO_4	108	18	>30	>30	30	2.3
Yes			1.8	15	12.5	25	2.1
No	SO_4^{2-}/$Al_2(SO_4)_3$	108	17.8	>30	>30	>30	n.a.
Yes			1.8	15	12.6	25	2.2

[a] Time to achieve the indicated conversion in minutes.
[b] Maximum allowed discharge limit for the wastewater discharged to sensitive areas (Council Directive 91/271/EEC concerning urban wastewater treatment).

as well as that of the suspended solids, on the ozonation of oxalic and mesoxalic acids was studied in pure water under catalysed and non-catalysed conditions at pH 8. In the case of bicarbonate, no sodium hydroxide was added to control pH during ozonation because of the buffering capacity of bicarbonate. The concentration used for each of these inorganic anions was the average of the values encountered in the same STP effluent in a previous one-year study [32]. These are shown in Table 2, together with the reaction time required to achieve 50% and 100% conversion of both acids and the anion source. Fig. 5a and b give the elimination profile of oxalic and mesoxalic acids, respectively, under non-catalysed reactions. Fig. 5c and d shows the depletion of mesoxalic and oxalic acids under catalytic ozonation.

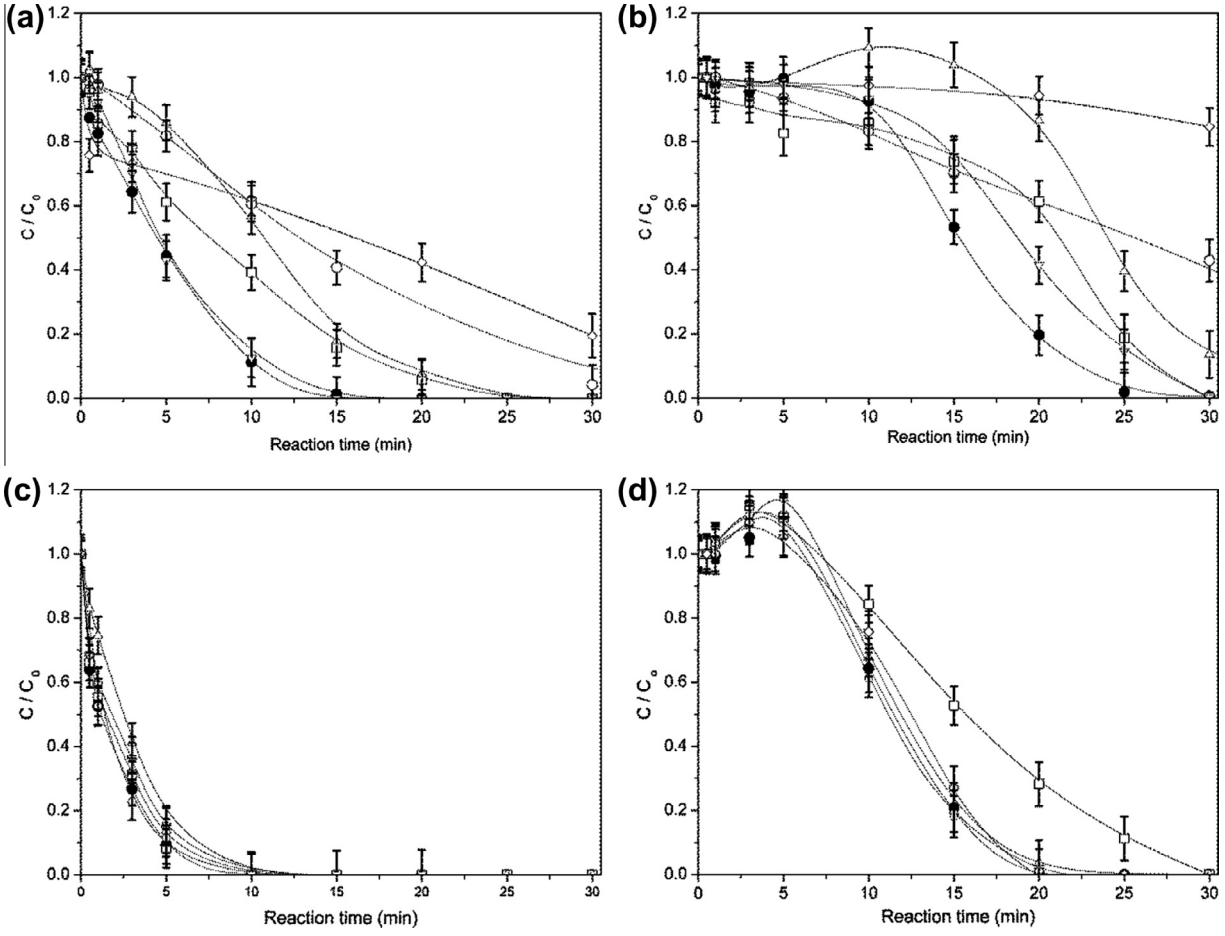

Fig. 5. Study of the influence of different parameters in the ozonation of mesoxalic acid (a, c) and oxalic acid (b, d) at pH 8 under non-catalytic (a, b) and catalytic (c, d) conditions. Symbols: (●) pure water, (○) bicarbonates, (□) phosphates, (▽) sulphates, (△) chloride, (◇) suspended solids. Error bars represent the standard deviation of sample replicates.

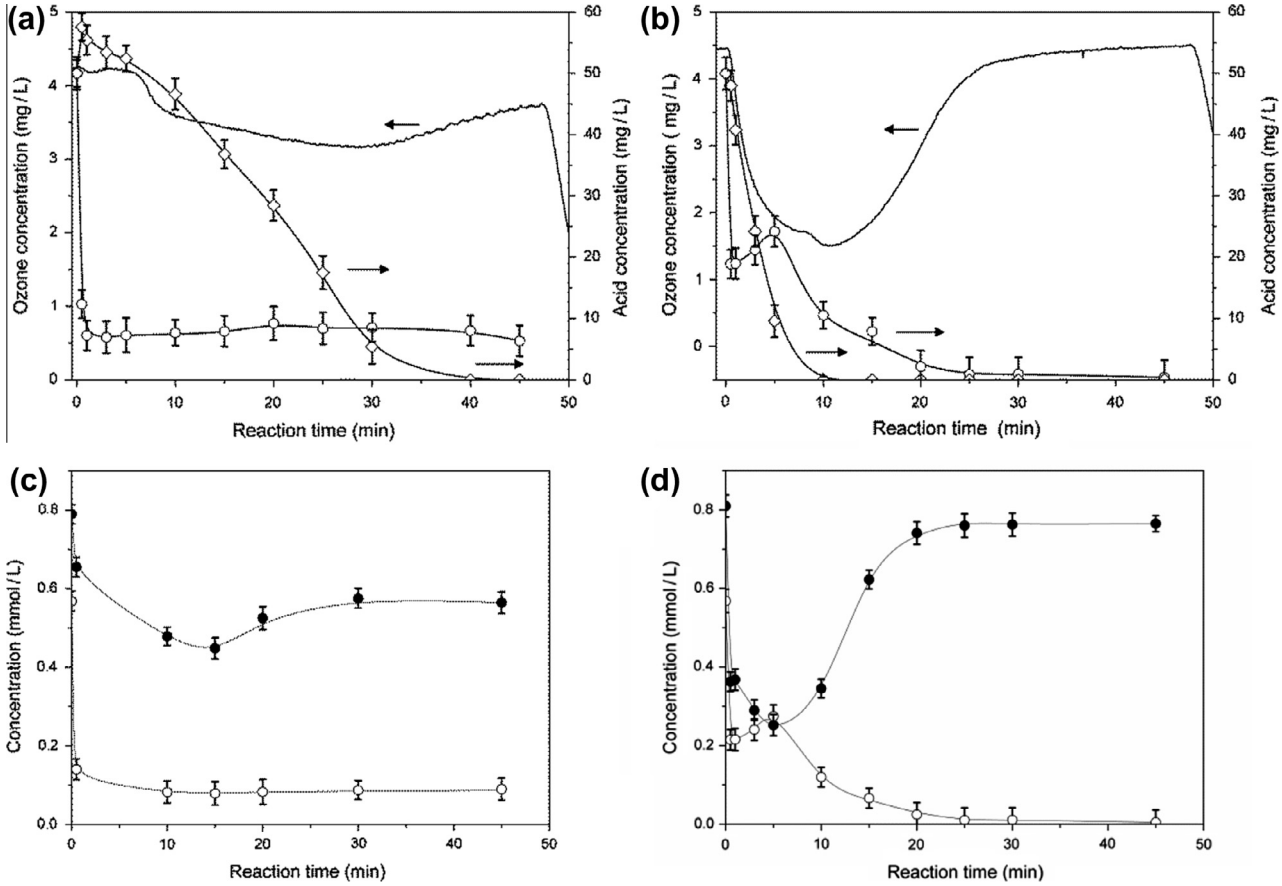

Fig. 6. Evolution of mesoxalic acid (◇), oxalic acid (○) and ozone (solid line) in wastewater matrix in non-catalysed reaction (a) and catalysed reaction (b). Evolution of calcium (●) and oxalic acid (○) in non-catalytic (c) and catalytic conditions (d). Error bars represent the standard deviation of sample replicates.

Non-catalysed reactions were strongly influenced by the presence of the different parameters studied. The effects followed the order SS > bicarbonates ≈ Cl^- > phosphates >> sulphates. The marked effect of bicarbonates ubiquitously present in natural waters was particularly noticeable; after 30 min, the oxalic acid was not fully depleted and the mesoxalic acid half-life as well as its total depletion time was twice as high as the figures obtained for pure water. The presence of chloride also negatively affects the depletion of both acids, exerting one of the strongest effects; however, its concentration (2.8 mmol/L) was very high. The effect of phosphate was also strong in spite of the low concentration (0.01 mmol/L). The results obtained suggest that under non-catalytic reaction, both acids are probably oxidised mainly by the hydroxyl radicals; the anions mentioned above to a greater or lesser extent, have been recognised as radical scavengers [21,56–58] and their presence could affect the indirect reaction pathway. The presence of sulphate (using sodium sulphate as source) did not affect the non-catalytic depletion of mesoxalic acid, and the reaction of oxalic acid was only slightly affected. In spite of the relatively high sulphate concentration (1.1 mmol/L), this small effect was the result of the negligible radical scavenger effect of sulphate [15].

The influence of suspended solids was studied using aluminium sulphate, a widely used coagulant in water treatment. This compound was chosen after determining that the sulphate anion did not modify the ozonation kinetics of either organic acid. At the working pH, the aluminium cation forms insoluble aluminium hydroxide particles. In the experiments, the withdrawn samples were immediately filtered using a Teflon 0.45 μm filter. The non-catalytic reaction of oxalic acid was almost suppressed and the mesoxalic acid reaction was severely slowed down. The negative effect of suspended solids on ozonation and their scavenger effect have previously been reported [59].

Catalysed reactions are only slightly slowed down by the presence of the anions and suspended solids studied, with the most noticeable effect being that exerted by phosphates on oxalic acid depletion. In all cases, the same profile was observed that in the reaction carried out in pure water, which consisted of an increase in oxalic acid concentration during mesoxalic depletion, indicating that the mechanism does not appear to change. It is notable that the increase in oxalic concentration in the anion matrix reaction started earlier than in pure water, probably due to the negative effect of the anion on the radical reaction pathway in favour of the catalytic one. The concentration of phosphates, sulphates and chlorides remained almost constant during the experiment, indicating that no significant adsorption of these anions took place on the catalyst surface, that means the catalytic active centre poisoning should be very low and hence the catalytic ozonation process it is not affected. The presence of suspended solids was almost unaffected by the presence of particulate matter in spite of the huge amount of suspended solids generated.

Table 2 shows the molar ratio of consumed ozone/organic acid depletion. In all the runs, the factor was lower for the catalytic one, indicating better performance of ozone in the catalytic process. Under catalytic reactions, no significant differences were found among the different runs, and the molar ratio was slighter higher than 2. Ozone consumption in non-catalytic reactions is more strongly influenced by the presence of inorganic anions, the scavenger capacity and concentration of which increase the ozone consumed, according to the previously mentioned scale.

3.5. STP effluent

The effect of a real wastewater matrix was studied in catalytic and non-catalytic runs using wastewater from the STP of Alcala de Henares spiked with oxalic and mesoxalic acids. The evolution of both acids and ozone are shown in Fig. 6 (6a for non-catalytic reactions and 6b for catalytic runs). The concentration of mesoxalic acid decreased continuously with reaction time, presenting a profile similar to that already described previously. Under non-catalytic conditions, approximately 40 min were required for its total depletion, which was similar to the reaction time found when assaying individual anions. The effect of the mixture and the presence of other compounds did not slow the ozonation reaction of mesoxalic acid down, the depletion rate being determined by the concentration of bicarbonate and phosphate. In catalytic runs, the total removal of mesoxalic acid was achieved in 10 min, a time similar to that found in pure water.

The ozonation of oxalic acid presented a remarkable feature, in that its concentration profile was different to that observed before and described in the preceding sections. In the first few minutes, the concentration decreased sharply (84% in non-catalytic runs) followed by a plateau that extended throughout the rest of the run in the absence of catalyst. These results can be explained by the presence of calcium cations (32 mg/L, see Table 1) in the wastewater matrix. Fig. 6c shows the evolution of the concentration of calcium and oxalic acid in a non-catalytic reaction. It can be seen that in parallel to oxalate, a sharp decrease in calcium concentration occurred. Calcium dropped from its initial value of 0.81 mmol/L to 0.48 mmol/L, while oxalate decreased from 0.57 mmol/L to 0.10 mmol/L. Although the precipitation equilibrium in a wastewater matrix is very complex and depends of several factors like temperature, pH, ionic strength, presence of DOC calcium oxalate is known to have a low solubility, 6.7 mg/L in pure water [60]. The disappearance of oxalate from the solution was probably due to precipitation rather than to oxidation. This was also supported by the fact that the consumption of ozone (0.8 mmol O_3/mmol organic acid, see Fig. 6a) was lower than that required for the complete oxidation of the organic acids, see Table 2. Fig. 6d depicts the evolution of oxalate and calcium in a catalytic run. In parallel to the initial oxalate depletion, a sharp decrease in calcium occurred, but during the second part of the reaction the concentration of calcium was restored. These results were also consistent with the previously indicated role of calcium oxalate; initially, a sharp decrease in oxalic acid (concurrently calcium) occurred due to fast precipitation of calcium oxalate, but since the elimination of the dissolved oxalate was produced by catalytic ozonation, the precipitate re-dissolved until the oxalic acid was completely eliminated and the initial calcium concentration was restored. The profile during the first part of the runs was complex, probably influenced by the oxidation of mesoxalic acid, the depletion of which corresponded to the maximum of oxalate observed in Fig. 6d.

4. Conclusions

The catalytic and non-catalytic ozonation of mesoxalic and oxalic acids was studied using CuO/SBA-15 as catalyst. The ozonation runs were performed at pH 8, close to the values usually found in wastewater, at which no significant leaching of the active phase took place. CuO/SBA-15 increased the rate of oxidation of both acids and reduced their overall depletion time by one third. The presence of inorganic anions, namely sulphate, phosphate, chloride and bicarbonate was studied. With the exception of sulphate, the inorganic anions reduced the rate of non-catalytic ozonation, most probably due to their role as scavenging hydroxyl radicals. In contrast, the influence of these anions on catalytic reactions was negligible. The presence of particulate matter inhibited the non-catalysed reaction of both acids, but the catalytic process was unaffected. The use of a wastewater effluent as matrix resulted in a reduction of the ozonation rate of mesoxalic acid in non-catalytic runs, essentially determined by the scavenging role of bicarbonate and phosphate. The concentration of oxalic acid was sharply reduced to 80% of its initial value during the first few seconds of the ozonation runs. The apparent oxalate depletion was attributed to calcium oxide precipitation. Using CuO/SBA-15 as catalyst, both acids could be effectively removed, and although calcium oxalate precipitation occurred, the dissolved oxalate was oxidised by catalytic ozonation until it was completely removed and the initial calcium concentration was restored.

References

[1] F.J. Beltrán, F.J. Rivas, R. Montero-de-Espinosa, Iron type catalysts for the ozonation of oxalic acid in water, Water Res. 39 (2005) 3553–3564.
[2] T. Asano, F.L. Burton, H.L. Leverenz, R. Tsuchihashi, G. Tchobanoglous, Water Reuse: Issues, Technologies, and Applications, McGraw Hill, New York, 2006.
[3] P. Paraskeva, N.J.D. Graham, Ozonation of municipal wastewater effluents, Water Environ. Res. 74 (2002) 569–581.
[4] R. Rosal, A. Rodríguez, J.A. Perdigón-Melón, M. Mezcua, M.D. Hernando, P. Letón, E. García-Calvo, A. Agüera, A.R. Fernández-Alba, Removal of pharmaceuticals and kinetics of mineralization by O_3/H_2O_2 in a biotreated municipal wastewater, Water Res. 42 (2008) 3719–3728.
[5] N. Funamizu, M. Kanno, T. Takakuwa, Measurement of bacterial growth potential in a reclaimed water, in: Water, Sanitation and Health: Resolving Conflicts between Drinking Water Demands and Pressures from Society's Waste, Bad Elster, Germany, 1998, pp. 281–286.
[6] F.J. Beltrán, J.F. García-Araya, I. Giráldez, Gallic acid water ozonation using activated carbon, Appl. Catal. B: Environ. 63 (2006) 249–259.
[7] J. Nawrocki, J. Świetlik, U. Raczyk-Stanisławiak, A. Dąbrowska, S. Biłozor, W. Ilecki, Influence of ozonation conditions on aldehyde and carboxylic acid formation, Ozone-Sci. Eng. 25 (2003) 53–62.
[8] E.C. Wert, F.L. Rosario-Ortiz, D.D. Drury, S.A. Snyder, Formation of oxidation byproducts from ozonation of wastewater, Water Res. 41 (2007) 1481–1490.
[9] B. Kasprzyk-Horden, U. Raczyk-Stanisławiak, J. Świetlik, J. Nawrocki, Catalytic ozonation of natural organic matter on alumina, Appl. Catal. B: Environ. 62 (2006) 345–358.
[10] P. Thayanukul, F. Kurisu, I. Kasuga, H. Furumai, Evaluation of microbial regrowth potential by assimilable organic carbon in various reclaimed water and distribution systems, Water Res. 47 (2013) 225–232.
[11] A. Rodríguez,·R. Rosal, J.A. Perdigón-Melón, M. Mezcua, A. Agüera, M.D. Hernando, P. Letón, A.R. Fernández-Alba, E. García-Calvo, Ozone-based technologies in water and wastewater treatment, in: D. Barceló, A.G. Kostianoy (Eds.), The Handbook of Environmental Chemistry, Springer-Verlag, Berlin, 2008, pp. 127–175.
[12] D.S. Pines, D.A. Reckhow, Solid phase catalytic ozonation process for the destruction of a model pollutant, Ozone-Sci. Eng. 25 (2003) 25–39.
[13] J. Staehelin, J. Hoigné, Decomposition of ozone in water in the presence of organic solutes acting as promoters and inhibitors of radical chain reactions, Environ. Sci. Technol. 19 (1985) 1206–1213.
[14] U. von Gunten, Ozonation of drinking water: Part I. Oxidation kinetics and product formation, Water Res. 37 (2003) 1443–1467.
[15] J. Hoigné, Chemistry of aqueous ozone and transformation of pollutants by ozonation and advanced oxidation processes, in: J. Hrubec (Ed.), The Handbook of Environmental Chemistry, Springer-Verlag, Berlin, 1998, pp. 84–137.
[16] T. Zhang, W. Li, J.P. Croué, A non-acid-assisted and non-hydroxyl-radical-related catalytic ozonation with ceria supported copper oxide in efficient oxalate degradation in water, Appl. Catal. B: Environ. 121–122 (2012) 88–94.
[17] G. Centi, S. Perathoner, Use of solid catalysts in promoting water treatment and remediation technologies, in: J.J. Spivey (Ed.), Catalysis, The Royal Society of Chemistry, Cambridge, 2005, pp. 46–71.
[18] J. Nawrocki, B. Kasprzyk-Horden, The efficiency and mechanism of catalytic ozonation, Appl. Catal. B: Environ. 99 (2010) 27–42.
[19] R. Rosal, M.S. Gonzalo, A. Rodríguez, J.A. Perdigón-Melón, E. García-Calvo, Catalytic ozonation of atrazine and linuron on MnO_x/Al_2O_3 and MnO_x/SBA-15 in a fixed bed reactor, Chem. Eng. J. 165 (2010) 806–812.
[20] F.J. Beltrán, F.J. Rivas, L.A. Fernández, P.M. Álvarez, R. Montero-de-Espinosa, Kinetics of catalytic ozonation of oxalic acid in water with activated carbon, Ind. Eng. Chem. Res. 41 (2002) 6510–6517.
[21] Y. Pi, M. Ernst, J.C. Schrotter, Effect of phosphate buffer upon CuO/Al_2O_3 and Cu(II) catalyzed ozonation of oxalic acid solution, Ozone-Sci. Eng. 25 (2003) 393–397.
[22] B. Legube, N. Karpel Vel Leitner, Catalytic ozonation: a promising advanced oxidation technology for water treatment, Catal. Today 53 (1999) 61–72.

[23] F.J. Rivas, M. Carbajo, F.J. Beltrán, B. Acedo, O. Gimeno, Perovskite catalytic ozonation of pyruvic acid in water operating conditions influence and kinetics, Appl. Catal. B: Environ. 62 (2006) 93–103.
[24] R. Rosal, A. Rodríguez, M.S. Gonzalo, E. García-Calvo, Catalytic ozonation of naproxen and carbamazepine on titanium dioxide, Appl. Catal. B: Environ. 84 (2008) 48–57.
[25] Q. Lu, F. Gao, S. Komarneni, T.E. Mallouk, Ordered SBA-15 nanorod arrays inside a porous alumina membrane, J. Am. Chem. Soc. 126 (2004) 8650–8651.
[26] A. Vinu, T. Mori, K. Ariga, New families of mesoporous materials, Sci. Technol. Adv. Mater. 7 (2006) 753–771.
[27] M.B. Lüchinger, Synthesis and functionalization of mesoporous silica and its application as a support for immobilized metal catalysts, Dissertation ETH Nr. 15847, Zürich, 2004.
[28] D. Zhao, J. Feng, Q. Huo, N. Melosh, G.H. Frederickson, B.F. Chmelka, G.D. Stucky, Triblock copolymer syntheses of mesoporous silica with periodic 50–300 angstrom pores, Science 279 (1998) 548–552.
[29] A.Y. Khodakov, V.L. Zholobenko, R. Bechara, D. Durand, Impact of aqueous impregnation on the long-range ordering and mesoporous structure of cobalt containing MCM-41 and SBA-15 materials, Micropor. Mesopor. Mater. 79 (2005) 29–39.
[30] M. Kruck, M. Jaroniec, C.H. Ko, R. Ryoo, Characterization of the porous structure of SBA-15, Chem. Mater. 12 (2000) 1961–1968.
[31] R.M. Rioux, H. Song, J.D. Hoefelmeyer, P. Yang, G.A. Somorjai, High-surface-area catalyst design: synthesis, characterization, and reaction studies of platinum nanoparticles in mesoporous SBA-15 silica, J. Phys. Chem. B. 109 (2005) 2192–2202.
[32] R. Rosal, A. Rodríguez, J.A. Perdigón-Melón, A. Petre, E. García-Calvo, M.J. Gómez, A. Agüera, A.R. Fernández-Alba, Occurrence of emerging pollutants in urban wastewater and their removal through biological treatment followed by ozonation, Water Res. 44 (2010) 578–588.
[33] K.S.W. Sing, Reporting Physisorption Data for Gas/Solid Systems with Special Reference to the Determination of Surface Area and Porosity, Pure & App. Chem. 57 (1985) 603–619.
[34] M.U.A. Prathap, B. Kaur, R. Srivastava, Direct synthesis of metal oxide incorporated mesoporous SBA-15, and their applications in non-enzymatic sensing of glucose, J. Colloid Interface Sci. 381 (2012) 143–151.
[35] A. Gervasini, S. Bennici, Dispersion and surface states of copper catalysts by temperature-programmed-reduction of oxidized surfaces (s-TPR), Appl. Catal. A: Gen. 281 (2005) 199–205.
[36] C.H. Tu, A.Q. Wang, M.Y. Zheng, X.D. Wang, T. Zhang, Factors influencing the catalytic activity of SBA-15-supported copper nanoparticles in CO oxidation, Appl. Catal. A: Gen. 297 (2006) 40–47.
[37] Y. Wang, H. Chu, W. Zhu, Q. Zhang, Copper-based efficient catalysts for propylene epoxidation by molecular oxygen, Catal. Today 131 (2008) 496–504.
[38] H. Zhang, C. Tang, Y. Lv, C. Sun, F. Gao, L. Dong, Y. Chen, Synthesis, characterization, and catalytic performance of copper-containing SBA-15 in the phenol hydroxylation, J. Colloid Interface Sci. 380 (2012) 16–24.
[39] P. Kuśtrowski, L. Chmielarz, R. Dziembaj, P. Cool, E.F. Vansant, Dehydrogenation of ethylbenzene with nitrous oxide in the presence of mesoporous silica materials modified with transition metal oxides, J. Phys. Chem. A 109 (2005) 330–336.
[40] Q. Gao, W. Xu, Y. Xu, D. Wu, Y. Sun, F. Deng, W. Shen, Amino acid adsorption on mesoporous materials: influence of types of amino acids, modification of mesoporous materials, and solution conditions, J. Phys. Chem. B 112 (2008) 2261–2267.
[41] M. Kokunešoski, J. Gulicovski, B. Matović, M. Logar, S.K. Milonjić, B. Babić, Synthesis and surface characterization of ordered mesoporous silica SBA-15, Mater. Chem. Phys. 124 (2010) 1248–1252.
[42] T. Ben-Moshe, I. Dror, B. Berkowitz, Oxidation of organic pollutants in aqueous solutions by nanosized copper oxide catalysts, Appl. Catal. B: Environ. 85 (2009) 207–211.
[43] J.A. Lewis, Colloidal processing of ceramics, J. Am. Ceram. Soc. 83 (2000) 2341–2359.
[44] J. Hoigné, H. Bader, The role of hydroxyl radical reactions in ozonation processes in aqueous solutions, Water Res. 10 (1976) 377–386.
[45] J. Hoigné, H. Bader, Rate constants of reactions of ozone with organic and inorganic compounds in water-II: dissociating organic compounds, Water Res. 17 (1983) 185–194.
[46] J. Prado, J. Arantegui, E. Chamarro, S. Esplugas, Degradation of 2,4-D by ozone and light, Ozone-Sci. Eng. 16 (1994) 235–245.
[47] J. Hoigné, Inter-calibraiton of OH radical sources and water quality parameters, Water Sci. Technol. 35 (1997) 1–8.
[48] D.S. Pines, D.A. Reckhow, Effect of dissolved cobalt (II) on the ozonation of oxalic acid, Environ. Sci. Technol. 36 (2002) 4046–4051.
[49] P. Fordham, M. Besson, P. Gallezot, Catalytic oxidation with air of tartronic acid to mesoxalic acid on bismuth-promoted platinum, Catal. Lett. 46 (1997) 195–199.
[50] T. Mallat, A. Baiker, Oxidation of alcohols with molecular oxygen on platinum metal catalysts in aqueous solutions, Catal. Today 19 (1994) 247–283.
[51] S. Kang, B. Xing, Adsorption of dicarboxylic acids by clay minerals as examined by in situ ATR-FTIR and ex situ DRIFT, Langmuir 23 (2007) 7024–7031.
[52] P. Santos, A. Yustos, G. Quintanilla, F. Ruiz, A. Garcia-Ochoa, P. Santos, A. Yustos, G. Quintanilla, F. Ruiz, Garcia-Ochoa Study of the copper leaching in the wet oxidation of phenol with CuO-based catalysts: causes and effects, Appl. Catal. B: Environ. 61 (2005) 323–333.
[53] A. Alejandre, F. Medina, A. Fortuny, P. Salagre, J.E. Sueiras, Characterisation of copper catalysts and activity for the oxidation of phenol aqueous solutions, Appl. Catal. B: Environ. 16 (1998) 53–67.
[54] U. Jans, J. Hoigné, Activated carbon and carbon black catalyzed transformation of aqueous ozone into OH-radicals, Ozone-Sci. Eng. 20 (1998) 67–90.
[55] F.J. Beltrán, J. Rivas, P. Álvarez, R. Montero-de-Espinosa, Kinetics of heterogeneous catalytic ozone decomposition in water on an activated carbon, Ozone-Sci. Eng. 24 (2002) 227–237.
[56] R. Andreozzi, V. Caprio, A. Insola, R. Marotta, V. Tufano, The ozonation of pyruvic acid in aqueous solutions catalyzed by suspended and dissolved manganese, Water Res. 32 (1998) 1492–1496.
[57] M.S. Siddiqui, Chlorine-ozone interactions: formation of chlorate, Water Res. 30 (1996) 2160–2170.
[58] G.V. Buxton, C.L. Greenstock, W.P. Helman, A.B. Ross, Critical review of rate constants for reactions of hydrated electrons, hydrogen atoms and hydroxyl radicals (·OH/·OH^-) in aqueous solution, J. Phys. Chem. Ref. Data 17 (1988) 513–886.
[59] A. Lopez, C. Di Iaconi, G. Mascolo, A. Pollice, Innovative and Integrated Technologies for the Treatment of Industrial Wastewater (INNOWATECH), IWA Publishing, London, 2012.
[60] D.R. Lide, CRC Handbook of Chemistry and Physics, 89th ed., CRC Press, London, 2008.